

## In situ study of electric field controlled ion transport in the Fe/BaTiO<sub>3</sub> interface

Merkel, D. G.; Bessas, D.; Bazsó, G.; Jafari, A.; Rüffer, R.; Chumakov, A. I.; Khanh, N. Q.; Sajti, Sz; Celse, J. P.; Nagy, D. L.

**DOI**

[10.1088/2053-1591/aaa16c](https://doi.org/10.1088/2053-1591/aaa16c)

**Publication date**

2018

**Document Version**

Final published version

**Published in**

Materials Research Express

**Citation (APA)**

Merkel, D. G., Bessas, D., Bazsó, G., Jafari, A., Rüffer, R., Chumakov, A. I., Khanh, N. Q., Sajti, S., Celse, J. P., & Nagy, D. L. (2018). In situ study of electric field controlled ion transport in the Fe/BaTiO<sub>3</sub> interface. *Materials Research Express*, 5(1), Article 016405. <https://doi.org/10.1088/2053-1591/aaa16c><sup>3</sup>

**Important note**

To cite this publication, please use the final published version (if applicable).  
Please check the document version above.

**Copyright**

Other than for strictly personal use, it is not permitted to download, forward or distribute the text or part of it, without the consent of the author(s) and/or copyright holder(s), unless the work is under an open content license such as Creative Commons.

**Takedown policy**

Please contact us and provide details if you believe this document breaches copyrights.  
We will remove access to the work immediately and investigate your claim.

PAPER

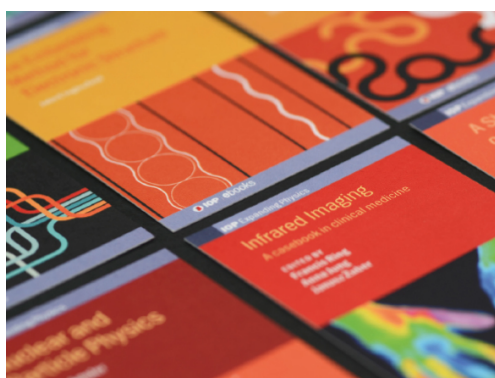
## *In situ* study of electric field controlled ion transport in the Fe/BaTiO<sub>3</sub> interface

To cite this article: D G Merkel *et al* 2018 *Mater. Res. Express* **5** 016405

View the [article online](#) for updates and enhancements.

### Related content

- [Electric field control of magnetic properties and electron transport in BaTiO<sub>3</sub>-based multiferroic heterostructures](#)  
M Asa, L Baldrati, C Rinaldi *et al.*
- [Quantification of charge-to-strain mediated interface coupling transfiguration in FE/FSMA multiferroic heterostructures](#)  
Kirandeep Singh and Davinder Kaur
- [Electrical control of magnetism in oxides](#)  
Cheng Song, Bin Cui, Jingjing Peng *et al.*



**IOP | ebooks™**

Bringing together innovative digital publishing with leading authors from the global scientific community.

Start exploring the collection—download the first chapter of every title for free.

# Materials Research Express



## PAPER

# *In situ* study of electric field controlled ion transport in the Fe/BaTiO<sub>3</sub> interface

RECEIVED  
10 November 2017

REVISED  
5 December 2017

ACCEPTED FOR PUBLICATION  
13 December 2017

PUBLISHED  
9 January 2018

D G Merkel<sup>1,2,6</sup> , D Bessas<sup>2,3</sup>, G Bazsó<sup>1</sup>, A Jafari<sup>2,4</sup>, R Ruffer<sup>2</sup>, A I Chumakov<sup>2</sup>, N Q Khanh<sup>5</sup>, Sz Sajti<sup>1</sup> , J-P Celse<sup>2</sup> and D L Nagy<sup>1</sup>

<sup>1</sup> Wigner Research Centre for Physics, Hungarian Academy of Sciences, H-1525 Budapest, Hungary

<sup>2</sup> European Synchrotron Radiation Facility, 71 avenue des Martyrs, CS 40220, F-38043 Grenoble Cedex 9, France

<sup>3</sup> Department of Radiation Science and Technology, Delft University of Technology, Mekelweg 15, 2629 JB Delft, The Netherlands

<sup>4</sup> DTU Space—National Space Institute, Technical University of Denmark, DK-2800 Kgs. Lyngby, Denmark

<sup>5</sup> Centre for Energy Research, Institute of Technical Physics and Materials Science, PO Box 49, H-1525 Budapest, Hungary

<sup>6</sup> Author to whom any correspondence should be addressed

E-mail: [merkel.daniel@wigner.mta.hu](mailto:merkel.daniel@wigner.mta.hu)

**Keywords:** multiferroics, nuclear resonance scattering, thin film, BaTiO<sub>3</sub>, magnetism

## Abstract

Electric field controlled ion transport and interface formation of iron thin films on a BaTiO<sub>3</sub> substrate have been investigated by *in situ* nuclear resonance scattering and x-ray reflectometry techniques. At early stage of deposition, an iron-II oxide interface layer was observed. The hyperfine parameters of the interface layer were found insensitive to the evaporated layer thickness. When an electric field was applied during growth, a 10 Å increase of the nonmagnetic/magnetic thickness threshold and an extended magnetic transition region was measured compared to the case where no field was applied. The interface layer was found stable under this threshold when further evaporation occurred, contrary to the magnetic layer where the magnitude and orientation of the hyperfine magnetic field vary continuously. The obtained results of the growth mechanism and of the electric field effect of the Fe/BTO system will allow the design of novel applications by creating custom oxide/metallic nanopatterns using laterally inhomogeneous electric fields during sample preparation.

## Introduction

The development of more advanced devices which can reflect upon the challenges of our world requires the exploration of novel material properties. Special systems which combine magnetic and electronic properties into a multifunctional material are excellent subject of this demand.

In multiferroic materials (in short *multiferroics*) the coexistence and coupling of ferroelectric [1] and magnetic order enables the fine control and modulation of electric polarization by magnetic field (*direct magnetoelectric effect, ME*) or the magnetic field by electric polarization (*converse magnetoelectric effect*) [2]. The electric field control of magnetic spin will lead to significantly lower energy consumption in actuators, information storage and spintronics devices, a key issue for sustainable development [3–5]. Not only the reduction of energy consumption but also the production of energy from ambient sources such as vibrations, sound, radiofrequency waves, light, temperature gradients and also novel medical applications give new perspectives for multiferroic materials [6–13].

Although several compounds have been reported to exhibit (anti)ferromagnetism and ferroelectricity simultaneously (single-phase multiferroics) [14–20], it is apparent, that the customization of these systems is limited.

As an alternative, it is possible to create heterogeneous or composite multiferroic systems by combining ferromagnetic (FM) and ferroelectric (FE) thin films or by evaporating an FM layer on a FE substrate [21]. In the case of the strain-induced magnetoelectric (ME) effect [22], a mechanical coupling through the interface is required. If a magnetic field is applied to the magnetostrictive phase, it induces strain in the epitaxially evaporated ferroelectric thin film. Due to the piezoelectric effect, this strain alters the electric polarization of the

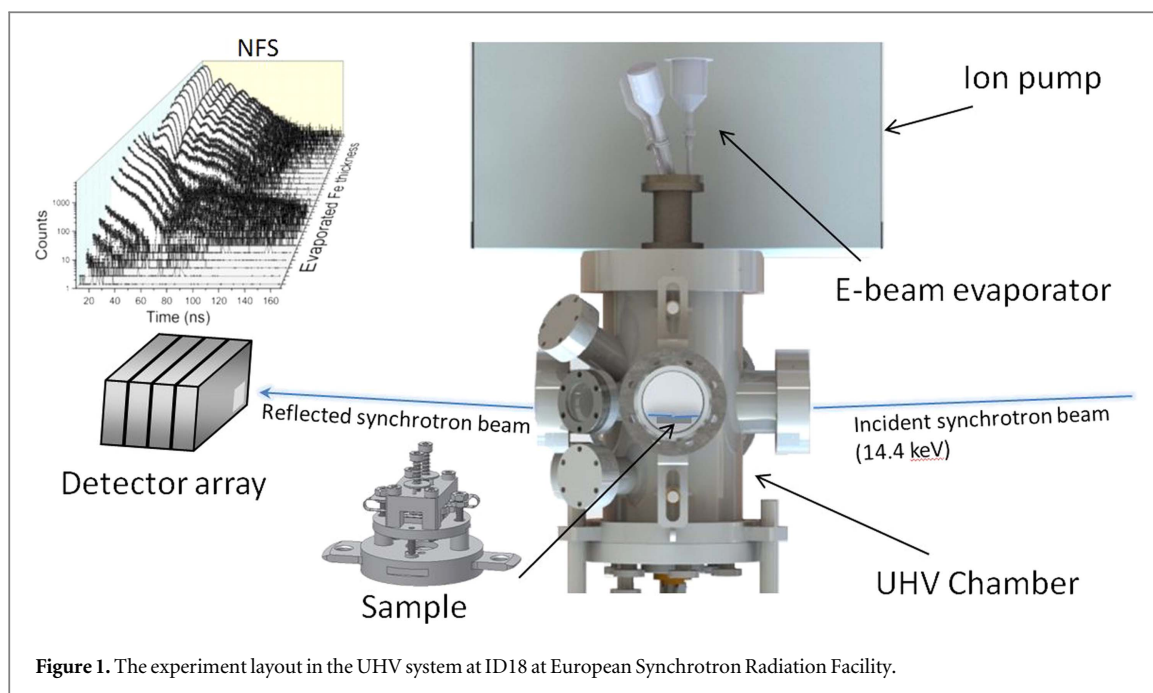


**Figure 1.** The experiment layout in the UHV system at ID18 at European Synchrotron Radiation Facility.

thin film, realizing the direct magnetoelastic coupling [23]. In the converse ME effect, the magnetic field is altered by electric polarization.

The Fe/BTO system, as a great example of strong ME coupling [24, 25] is an excellent system to investigate this phenomenon. Several works reported as well that an applied electric field can alter the properties of this system: Brivio and coworkers found major modifications of magnetic anisotropies and change in magnetic coercivity induced by the application of electric field [26]. Couet *et al* [27] reported that, if an electric field is applied to a Fe/BTO sample (above a certain threshold), the thickness of the iron oxide layer at the interface increased.

All these exciting effects were observed *ex situ*, but the presence of electric field during the sample growth (*in situ*) has never been investigated.

In the present work, we have performed an *in situ* comprehensive research on iron growth on BTO substrate with the application of electric field by using time resolved nuclear forward scattering (NFS) technique [28–30].

## Experiment

The experiment was carried out at the nuclear resonance beamline ID18 [31] at the European Synchrotron Radiation Facility (ESRF), using the nuclear resonant chamber of the in beam ultrahigh-vacuum system [32]. Iron-57 was evaporated from a rod mounted in a 4-pocket electron-beam evaporator (Oxford Applied Research) to a 5 mm × 5 mm × 0.5 mm BaTiO<sub>3</sub> substrate with (001) orientation (purchased from Alineason Materials Technology GmbH). The base pressure was in the order of 10<sup>-11</sup> mbar and increased to the 10<sup>-10</sup> mbar regime during evaporation and the sample temperature increased to 80 °C.

During deposition *in situ* NFS and x-ray reflectivity curves were recorded by using a four unit, avalanche photo diode detector system with nanosecond time resolution. The experiment was performed at 14.412 keV, the energy corresponding to the 1/2–3/2 nuclear transition of iron-57 with a beam of 0.5 meV resolution and focused by a Kirkpatrick-Baez mirror system both horizontally and vertically to 20 μm and 8.7 μm, respectively. The deposition rate was set extremely low to (0.02 Å min<sup>-1</sup>) in order to have enough time to measure reflectivity curves and time spectra at a given iron thickness range. The measurement layout is shown in figure 1. Two series of samples were measured, one without and the other with electric field created by a 1 kV potential difference between the top and bottom electrode.

The electric field was applied to the sample using a special sample holder; see figure 2. The lower gold electrode was sputtered on a 12 mm × 12 mm × 1.5 mm Al<sub>2</sub>O<sub>3</sub> ceramic plate. The BTO substrate was pressed against this electrode by four 1 mm diameter ZrO<sub>2</sub> glass rods. The iron-57 atoms reached the surface through a 3.5 mm × 1 mm slot milled in the 1 mm thick Cu top electrode which was 0.5 mm above the top of the substrate. Through the experiment negative voltage was applied to the lower electrode while the upper contact was grounded.

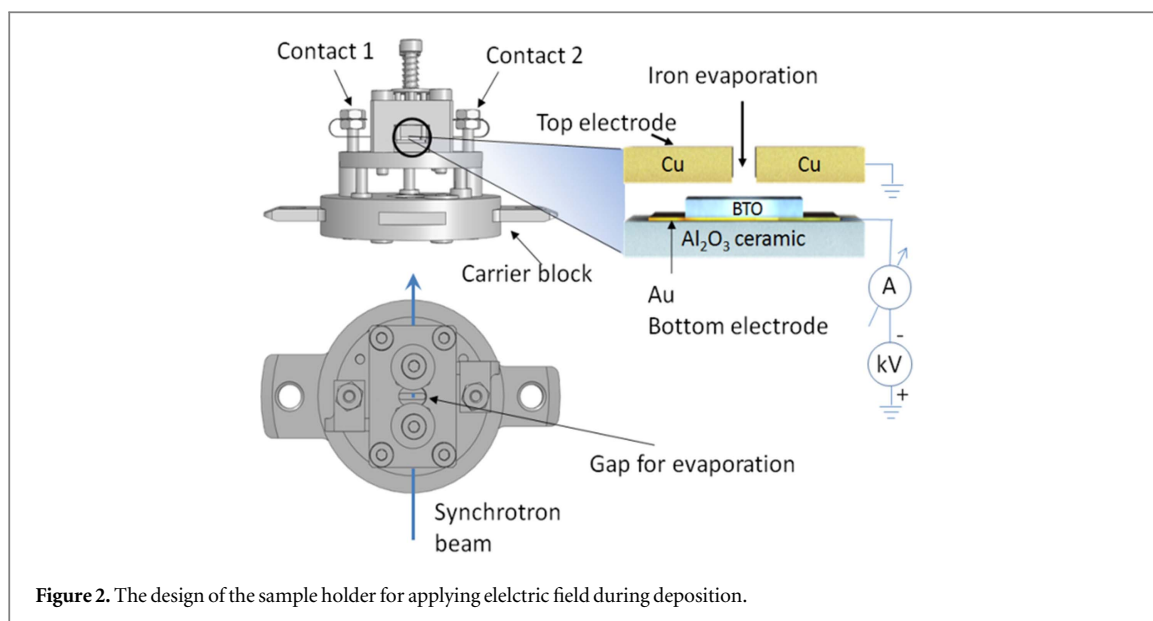


Figure 2. The design of the sample holder for applying electric field during deposition.

Although the top surface of the sample was not directly connected to the top electrode during the deposition, the conduction of the x-ray produced photoelectrons ensured that the potential difference between the top of the sample, and the top electrode vanished in a few seconds. The charging current pulse was registered from the picoammeter (about 4 nA peak), when the x-ray shutter was opened, and the total charge was found to be commensurable with the product of the applied voltage and the capacity calculated from the geometrical parameters and the relative permittivity of the substrate.

The evaluation of NFS data was done by using the free program FitSuite [33].

## Results

From the evaluation of the NFS data the variation of iron hyperfine parameters were determined for a given evaporated thickness. In figure 3, the *in situ* recorded time spectra are shown as a function of the deposited iron thickness in case of 0 V and 1 kV applied voltage, respectively. Below the 2D intensity plot, selected NFS spectra corresponding to a given thickness are shown. Isomer shifts (IS) were determined relative to the metallic iron layer when it appeared and the same values were used for lower thicknesses without metallic iron. In case of no applied electric field and below 25.1(2) Å thickness, the spectra could be fitted by two doublets, with a relatively large isomer shift (both IS = 1.0(1) mm s<sup>-1</sup>) and with quadrupole splitting QS = 0.69–0.72 mm s<sup>-1</sup> and QS = 1.1–1.4 mm s<sup>-1</sup>. These values can be associated to iron(II) oxide [34, 35] in case of bulk and for iron(II) atoms in the vicinity of vacancies and defect clusters, respectively. Initially, the lower QS site contributed 82% to the spectrum and increased up to 94% (within the oxide components) by the thickest layer. The first magnetic oscillation appeared in the spectrum at 26.9(4) Å deposited layer thickness with a highly reduced and highly distributed hyperfine (HF) magnetic field (HMF) of 19 T (median value of HMF distribution) aligned 58(2)<sup>o</sup> relative to the sample surface normal. On the way to 60 Å, the width of the HMF distribution decreased and the HMF slowly converges to the bulk value of iron, reaching 31.8 T by the thickest layer. In case, when 1 kV voltage was applied during layer growth, the nonmagnetic regime (below 35.7(3) Å) could be fitted by the same two doublets, as it was for the 0 V sample. Also the inset of magnetization shows similar behavior to the 0 V sample. The observation of high frequency oscillations at 35.7(3) Å is due to 19 T hyperfine magnetic field with the orientation of 67(2)<sup>o</sup> to the surface normal. With the growth of iron, the magnetic moments turned in plane and a continuous increase in the HMF could be observed. As opposed to the previous example, the slope of HMF augmentation remained approximately constant up to the highest 60.8(5) Å, where the median hyperfine magnetic field was found to be 29.6 T. It can be seen that the electric field has great effect on iron oxidation during deposition.

## Discussion

Figure 4 summarize the properties of two samples at various steps of the deposition process. The extracted median value and orientation (relative to the sample surface) of the hyperfine magnetic fields are shown as a function of evaporated iron thickness. At lower thicknesses, the interface layer reveals iron-II oxide with no

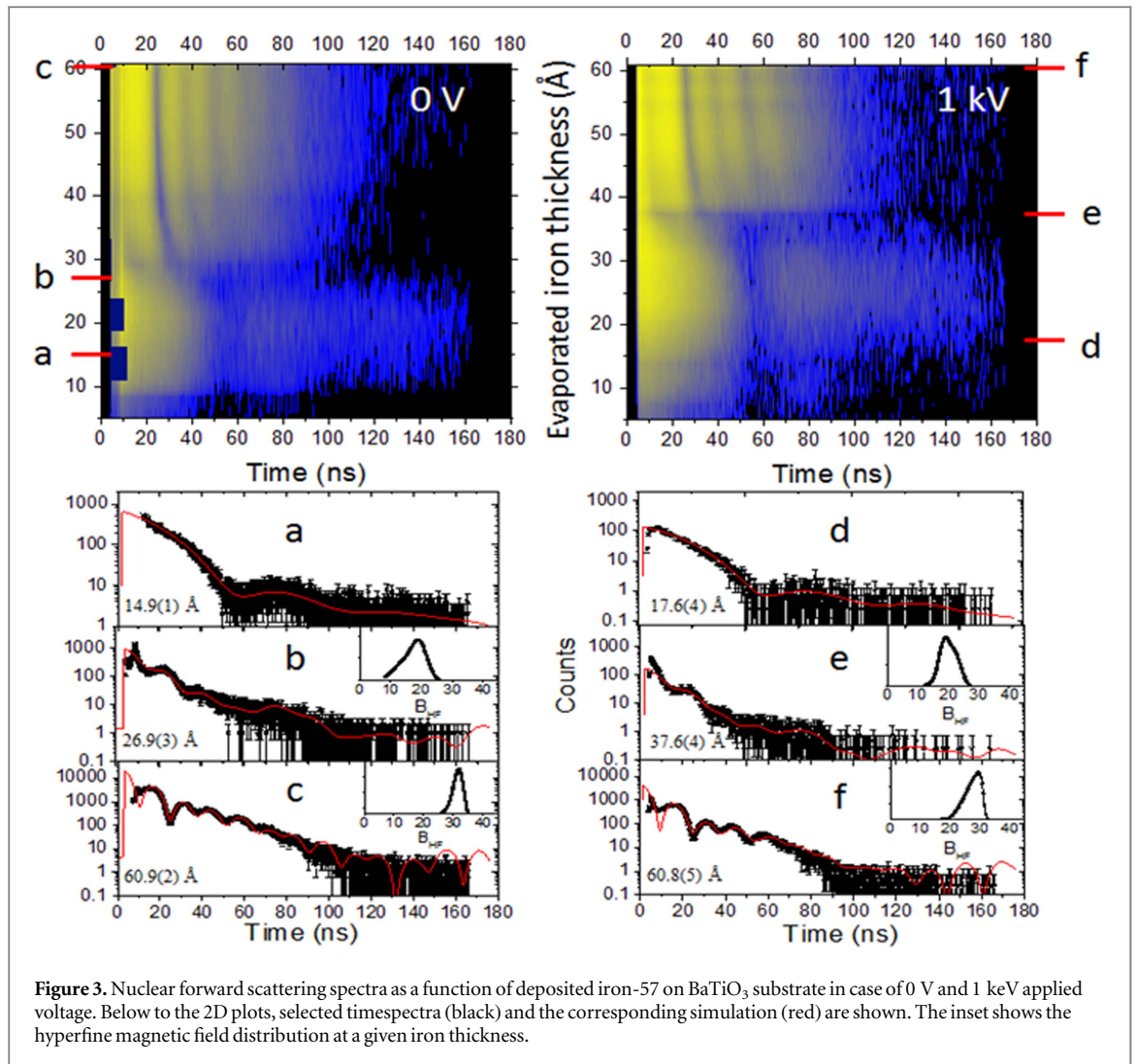


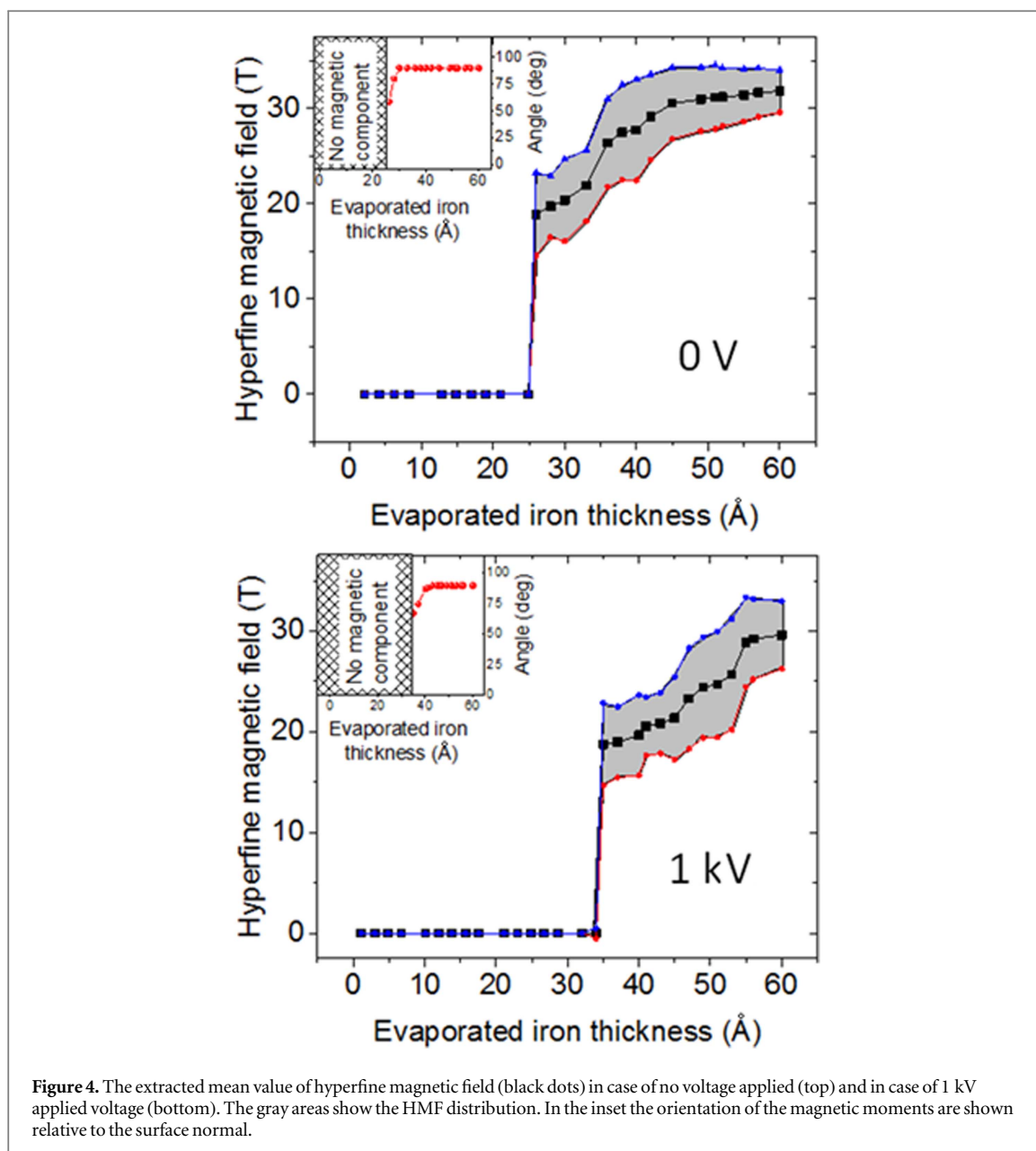
**Figure 3.** Nuclear forward scattering spectra as a function of deposited iron-57 on BaTiO<sub>3</sub> substrate in case of 0 V and 1 keV applied voltage. Below to the 2D plots, selected timespectra (black) and the corresponding simulation (red) are shown. The inset shows the hyperfine magnetic field distribution at a given iron thickness.

ferromagnetic ordering, where the necessary oxygen injection was provided by the BTO substrate. According to the theory of Cabrera and Mott [36, 37], the electron can freely pass through the oxide layer from the metal side via tunneling or thermionic emission causing equilibration of the Fermi levels in the metal and the oxidizer layer. As a consequence, a uniform electric field arises—created by the positive Fe/FeO and negative FeO/BTO interface—and supports slow ionic transport across the interface. Without the presence of this electric field, the chance for an ion to go over the potential barrier  $U$ , would be  $\nu \exp(-U/kT)$ , with  $\nu$  being the atomic frequency of vibration  $k$  the Boltzmann constant and  $T$  the temperature. Following the derivation of Cabrera and Mott, if electric field arises, it lowers the potential barrier in the direction of the field by  $0.5qaE$ , increasing the probability of movement to  $\nu \exp(-(U - 0.5qaE)/kT)$ , with  $a$  being the interatomic distance,  $q$  the charge of the ion and  $E$  the electric field. In the other direction, however, the same field decreases the chance of movement by the same amount, resulting an ionic drift through the interface. Therefore, applying external electric field to the sample in the right direction is expected to enhance the formation of the interface layer.

The oxidation state of the deposited layer was found to be independent on the thickness of the evaporated layer. On the other hand, as discussed above, we observed a change in the ratio of the QS components. This reveals the reduction of vacancies and defect clusters in the growing interface.

Furthermore, we found that, for both 1 kV and 0 V samples, the position of the boundary between the nonmagnetic and magnetic layers does not move with the increasing of the thickness of the magnetic layer. This suggests that once the metallic iron appears, the oxygen diffusion through the interface is hindered, and no further oxidation occurs. Thus, the additional iron deposition has no influence on the most properties and the thickness of the non-magnetic interface layer.

For the Fe/BTO system, several thicknesses of the interface have been reported: Zenkevich *et al* 20 Å [38], Couet *et al* 6.5 Å [27], Brivio *et al* 30 Å [26]. In our case, it was found to be 26.9(3) Å for the 0 V sample. These differences may stem from the specific growth conditions, including growth rate, sample temperature and vacuum in the chamber.



When an external electric field was applied during deposition, we found  $\sim 10$  Å increase of the interface layer compared to the 0 V sample. A possible reason for this is the alteration of equilibrium conditions between the two opposite effects, which govern oxidation, namely: the uniform electric field in the interface (support slow oxygen transport) and the diffusion barrier which blocks oxygen transport. With the additional electric field an extra driving force was introduced, which is responsible for the elevated interface thickness.

Contrary to most of the properties of the non-magnetic interface, those of the magnetic layer change during deposition continuously (figure 4). With the appearance of ferromagnetic ordering, a mixing between oxide and metallic iron layer can be suggested, where small iron islands are separated by oxide, which explains the diminished HMF by superparamagnetic relaxation and the out of plane magnetic components by the low shape anisotropy. With further iron deposition the size of the islands increase, they coalesce, resulting an enhancement in the HMF. Where no external field was applied, this procedure affects the relatively narrow regime of 27–35 Å, and ends with a jump of HMF at  $\sim 35$  Å. With 1 kV applied voltage, this transition region starts at larger thickness ( $\sim 36$  Å), and a smoother increase of HMF occurs in the thickness range of 36 Å–55 Å (figure 4).

Thus, the *in situ* study of the growing interface reveals important details of the growth process. Such an understanding of interface formation and the electric field effect has great potential in novel applications. By applying inhomogeneous electric field during sample growth, the interface thickness can be tailored according to the demands and even, artificial lateral nanostructures can be built.

## Summary

*In situ* experiments have been performed, in order to investigate the ion transport during iron growth on a ferroelectric BaTiO<sub>3</sub> substrate, with and without applied external electric field. In a specially designed sample holder, 0 V and 1 kV was applied to the sample meanwhile NFS spectra and x-ray reflectivity curves were recorded. Below a certain thickness threshold, iron-II oxide interface layer was observed, and the hyperfine parameters in this layer were found to be insensitive to the evaporated layer thickness. We have observed that the magnetic component appeared at about 10 Å thicker layer in case of an external electric field due to the supported ion transfer through the interface and also an extended magnetic transition region was measured. Furthermore, we claim that neither the nonmagnetic/magnetic interface position alters with further deposition nor the properties of the non-magnetic interface layer are affected, contrary to the magnetic layer where the magnitude and orientation of hyperfine magnetic field vary continuously with increasing thickness. The comprehensive understanding of the growth mechanism, as well as the effect of the electric field on the Fe/BTO system can lead to novel applications by the application of laterally controlled electric field. This way, custom oxide/metallic nanopatterns can be designed which are of great importance of spintronics and nanotechnology.

## Acknowledgments

The European Synchrotron Radiation Facility is acknowledged for beamtime provision at the Nuclear Resonance Beamline ID18. DB acknowledges financial support from the Industrial Partnership Program (IPP-I28) of Foundation for Fundamental Research on Matter (FOM) (The Netherlands) and BASF New Business.

## ORCID iDs

D G Merkel  <https://orcid.org/0000-0001-9644-2521>

Sz Sajti  <https://orcid.org/0000-0002-8748-8242>

## References

- [1] Nuraje N and Su K 2013 *Nanoscale* **5** 8752
- [2] Wang Y, Hu J, Lin Y and Nan C-W 2010 *NPG Asia Mater.* **2** 61–8
- [3] Moodera J, Miao G-X and Santos T 2010 *Phys. Today* **63** 46
- [4] Ming L C 2010 *J. Appl. Phys.* **107** 09D918
- [5] Vopsaroiu M, Cain M G, Sreenivasulu G, Srinivasan G and Balbashov A M 2012 *Mater. Lett.* **66** 282
- [6] Palneedi H, Annareddy V, Priya S and Ryu J 2016 *Actuators* **5** 9
- [7] Patil D R, Zhou Y, Kang J-E, Sharpes N, Jeong D-Y, Kim Y-D, Kim K.H., Priya S. and Ryu J. 2014 *APL Mater.* **2** 046102
- [8] Ryu J, Kang J-E, Zhou Y, Choi S-Y, Yoon W-H, Park D-S, Choi J-J, Hahn B-D, Ahn C-W and Kim J-W 2015 *Energy Environ. Sci.* **8** 2402
- [9] Hockel J L, Bur A, Wu T, Wetzlar K P and Carman G P 2012 *Appl. Phys. Lett.* **100** 022401
- [10] Paluszek M, Avirovik D, Zhou Y, Kundu S, Chopra A, Montague R and Priya S 2015 *Magnetolectric composites for medical application Composite Magnetolectrics* ed G Srinivasan et al (Cambridge, UK: Woodhead Publishing) pp 297–327
- [11] Guduru R, Liang P, Runowicz C, Nair M, Atluri V and Khizroev S 2013 *Sci. Rep.* **3** 2953
- [12] Kargol A, Malkinski L and Caruntu G 2012 *Biomedical applications of multiferroic nanoparticles Advanced Magnetic Materials* ed L Malkinski (Rijeka, Croatia: InTech) pp 89–118
- [13] Shirokhar M M, Hao C, Dong X, Guo T, Zhang L, Li M and Wang H 2014 *Nanoscale* **6** 4735
- [14] Neaton J B, Ederer C, Waghmare U V, Spaldin N A and Rabe K M 2005 *Phys. Rev. B* **71** 014113
- [15] Kumar A and Varshney D 2012 *Ceram. Inter.* **38** 3935
- [16] Katsufuji T, Mori S, Masaki M, Moritomo Y, Yamamoto N and Takagi H 2001 *Phys. Rev. B* **64** 104419
- [17] Efremov D V, van den Brink J and Khomskii D I 2004 *Nat. Mater.* **3** 853
- [18] Cheong S W and Mostovoy M 2007 *Nat. Mater.* **6** 13
- [19] Seshadri R R and Hill N A 2001 *Chem. Mater.* **13** 2892
- [20] Kuo C-Y et al 2016 *Nat. Commun.* **7** 12712
- [21] Srinivasan G, Rasmussen E T, Levin B J and Hayes R 2002 *Phys. Rev. B* **65** 134402
- [22] Eerenstein W, Wiora M, Prieto J L, Scott J F and Mathur N D 2007 *Nat. Mater.* **6** 348
- [23] Scott J F 2007 *Nat. Mater.* **6** 256
- [24] Radaelli G et al 2014 *Nat. Commun.* **5** 3404
- [25] Garcia V et al 2010 *Science* **327** 1106
- [26] Brivio S, Petti D, Bertacco R and Cezar J C 2011 *Appl. Phys. Lett.* **98** 092505
- [27] Couet S, Bisht M, Trekels M, Menghini M, Petermann C, Van Bael M J, Locquet J-P, Ruffer R, Vantomme A and Temst K 2014 *Adv. Funct. Mater.* **24** 71
- [28] Merkel D G, Bessas D, Zolnai Z, Ruffer R, Chumakov A I, Paddubrouskaya H, Van Haesendonck C, Nagy B N, Tóth A L and Deák A 2015 *Nanoscale* **7** 12878
- [29] Erb D, Schlage K, Bocklage L, Hübner R, Merkel D G, Ruffer R, Wille H-C and Röhlberger R 2017 *Phys. Rev. Mater.* **1** 023001
- [30] Schlage K, Dzemiantsova L, Bocklage L, Wille H-C, Poes M, Meier G and Röhlberger R 2017 *Phys. Rev. Lett.* **118** 237204
- [31] Ruffer R and Chumakov A I 1996 *Hyperfine Interact.* **97** 589
- [32] Stankov S, Ruffer R, Sladeczek M, Rennhofer M, Sepiol B, Vogl G, Spiridis N, Ślęzak T and Korecki J 2008 *Rev. Sci. Instrum.* **79** 045108

- [33] Sajti S, Deák L and Bottyán L 2009 <http://fs.kfki.hu> (arXiv: 0907.2805)
- [34] Wilkinson C, Cheetham A K, Long G J, Battle P D and Hope D A O 1984 *Inorg. Chem.* **23** 3136
- [35] Koziol-Rachwał A, Ślęzak T, Nozaki T, Yuasa S and Korecki J 2016 *Appl. Phys. Lett.* **108** 041606
- [36] Cabrera N and Mott N F 1949 *Rep. Prog. Phys.* **12** 163
- [37] Atkinson A 1985 *Rev. Mod. Phys.* **57** 2
- [38] Zenkevich A, Mantovan R, Fanciulli M, Minnekaev M, Matveyev Y, Lebedinskii Y, Thiess S and Drube W 2010 *Appl. Phys. Lett.* **96** 162110